M R S Internet Journal Nitride Semiconductor Research

Structural and optical properties of GaN laterally overgrown on Si(111) by metalorganic chemical vapor deposition using an AlN buffer layer

H. Marchand[1], N. Zhang[1], L. Zhao[1], Y. Golan[1], S. J. Rosner[2], G. Girolami[2], Paul T. Fini [1], J.P. Ibbetson[1], S. Keller[1], Steven DenBaars [1], J. S. Speck[1] and U. K. Mishra[1]
[1]*Electrical and Computer Engineering and Materials Departments, University of California, Santa Barbara,*
[2]*Hewlett-Packard Laboratories, Palo Alto,*

(Received Thursday, February 11, 1999; accepted Wednesday, March 10, 1999)

Lateral epitaxial overgrowth (LEO) on Si(111) substrates using an AlN buffer layer is demonstrated and characterized using scanning electron microscopy, atomic force microscopy, transmission electron microscopy, x-ray diffraction, photoluminescence spectroscopy, and cathodoluminescence imaging. The <1$\bar{1}$00>-oriented LEO GaN stripes grown on silicon substrates are shown to have similar structural properties as LEO GaN grown on GaN/Al_2O_3 substrates: the surface topography is characterized by continuous crystallographic steps rather than by steps terminated by screw-component threading dislocations; the density of threading dislocations is $<10^6$ cm^{-2}; the LEO regions exhibit crystallographic tilt (0.7-4.7°) relative to the seed region. The AlN buffer thickness affects the stripe morphology and, in turn, the microstructure of the LEO GaN. The issues of chemical compability and thermal expansion mismatch are discussed.

1 Introduction

Lateral epitaxial overgrowth (LEO) is an attractive method to produce GaN films with a low density of extended defects, which is beneficial both to studies of the fundamental properties of the GaInAlN materials system and to GaN-based device technology. Recent studies have confirmed that the density of threading dislocations (TDs) is reduced by 3-4 orders of magnitude in the LEO material grown on 6H-SiC [1] and Al_2O_3 [2] [3] [4] substrates, and the mechanisms of threading dislocations evolution during LEO have been investigated. [1] [2] [4] [5] [6] Studies of the optical properties of LEO GaN [7] [8] [9] and InGaN quantum wells [7] [10] have revealed that TDs act as non-radiative recombination centers. However, the minority carrier diffusion length (<200 nm) is smaller than the average distance between TDs, [10] such that the emission mechanisms of the carriers that do recombine radiatively appear to be unaffected by moderate TD densities (~10^6-10^9 cm^{-2}). On the other hand, reducing the TD density has been shown to reduce the reverse leakage current by ~3 orders of magnitude in GaN p-n junctions , [11] InGaN single [12] and multiple [13] quantum well light emitting diodes, and GaN/AlGaN heterojunction field-effect transistors [14] fabricated on LEO GaN. More recently, ultraviolet p-i-n photodetectors fabricated on LEO AlGaN have exhibited a similar reduction of the reverse leakage current by up to 6 orders of magnitude. [15] The use of LEO GaN has also resulted in marked improvements in the lifetime of InGaN/GaN laser diodes. [16]

Such improvements in structural properties and device performance have revived interest in alternative substrates such as Si(111), which has potential advantages for device integration, thermal management, and cost. [17] [18] [19] For GaN on Si(111) in general, the difference in lattice parameters and the strength of the Si-N bond prevent the formation of smooth, single-crystal GaN. [20] [21] [22] This has been alleviated by using a two-step method involving various buffer layers such as SiC, [23] [24] GaN, [22] AlN, [17] [25] [26] [27] [28] [29] GaAs, [30] AlAs, [31] and SiN_x, [32] which typically yields a smooth morphology and a columnar microstructure with a TD density of 10^{10}-10^{11} cm^{-2}.

We have recently demonstrated a 3-4 orders of magnitude reduction of the TD density in LEO GaN grown on Si(111) using an intermediate AlN buffer layer partially covered by a SiO_2 mask. [33] GaN pyramids have

https://doi.org/10.1557/S1092578300000582 Published online by Cambridge University Press

also been fabricated on Si(111) by selective-area growth and LEO using an AlGaN buffer layer. [34] More recently GaN stripes were grown on etched GaN/AlN/SiC/Si(111) substrates [35] ('pendeo-epitaxy') and on SiO_2-patterned GaN/Si(111) layers; [36] however as of yet no analysis of the microstructural properties has been published.

In this paper we report on the structural and optical properties of GaN stripes grown on SiO_2-patterned AlN/Si(111) substrates using LEO. The extended defect reduction is characterized by transmission electron microscopy (TEM), x-ray diffraction (XRD), atomic force microscopy (AFM), and cathodoluminescence (CL) imaging. The optical properties are examined using CL and photoluminescence (PL) spectroscopy. It is shown that there is a relationship between the AlN buffer thickness and the stripe morphology which, in turn, affects the microstructure of the LEO GaN. Finally, the issues of chemical compability and thermal expansion mismatch are discussed.

2 Experimental

Two inch-diameter Si(111) wafers were etched in buffered HF for one minute before growth. After heating to the growth temperature of 900°C under hydrogen, the TMAl and NH_3 precursors were introduced in the metalorganic chemical vapor deposition (MOCVD) growth chamber and the AlN buffer layer was deposited at a total pressure of 76 Torr. The thickness of the AlN layer was ~60 nm ('sample A') or ~180 nm ('sample B'). In both cases the AlN layer was crack-free over the entire wafer, and the RMS roughness measured by AFM was on the order of 15 nm. [a] The wafers were then coated with 200 nm-thick SiO_2 using plasma-enhanced chemical vapor deposition, and 5 μm-wide stripes oriented in the $<1\bar{1}00>$ direction were patterned using standard UV photolithography and wet chemical etching. The width of the SiO_2 mask regions was 35 μm. The LEO regrowth was performed under the same conditions as in Ref. [3].

Samples were characterized by scanning electron microscopy (SEM) using a JEOL 6300F field emission microscope operating at 15 kV. Specimens for TEM were prepared by wedge polishing followed by standard Ar+ ion milling. Images were recorded on a JEOL 2000FX microscope operated at 200 kV. X-ray rocking curves were measured using Cu K_α radiation from a Bede double-crystal diffractometer. The surface topography was imaged using a Digital Instruments Dimension 3000 AFM operating in tapping mode. The room-temperature PL was excited using a HeCd laser (325 nm, ~20 mW/cm^2) and detected using a 1/8 m grating monochromator and a photomultiplier tube. The CL measurements were performed in a scanning electron microscope (SEM) at 10 kV (penetration depth of ~0.3-0.4 μm determined by Monte Carlo modeling) using an Oxford MonoCL mirror and grating spectrometer system for collecting the generated light and dispersing it to provide wavelength resolution. [38]

3 Results

Figure 1 shows cross-section SEM micrographs of typical LEO GaN stripes overgrown for 60 minutes from the SiO_2-masked AlN buffer layers. The 'seed' region corresponds to GaN grown vertically from the AlN buffer layer, whereas the 'LEO' regions correspond to GaN overgrown laterally over the SiO_2 mask, as indicated in Figure 1. The AlN buffer layer cannot be readily distinguished in Figure 1. For sample A (60 nm-thick AlN, Figure 1a) the stripe was bound on top by the (0001) facet and on the edges by vertical $\{11\bar{2}0\}$ facets and inclined sidewalls. The inclined sidewalls consist predominantly of the $\{11\bar{2}2\}$ facets but tend to break up into small facets which are most likely $\{1\bar{1}01\}$ 'pyramidal' facets. [39] [40] The stripes in sample B (180 nm-thick AlN, Figure 1b) are bound only by the (0001) facet and the inclined sidewalls.

Figure 2 shows the surface topography of samples A and B measured by AFM. Figure 2a is a wide-area image (144 μm^2) covering the seed and LEO regions of sample A. The topography of the seed region is dominated by c/2-height steps which tend to form partial spirals due to the high density (~2×10^9 cm^{-2}) of pure screw (Burgers vector **b** = <0001>) and mixed character (**b** = 1/3 $<11\bar{2}3>$) TDs and the high surface mobility of adsorbed species during growth. These TDs can be unambiguously located at the termination of c/2-height steps, [41] and are also usually associated with a small surface depression ~20 nm in diameter (see arrow "S" in Figure 2b). The LEO regions in Figure 2a are free of step terminations, which unambiguously shows that the density of screw-component TDs at the surface of the LEO GaN is markedly reduced compared to the seed region. For the 3 μm-wide LEO region in Figure 2a, one obtains ~3×10^6 cm^{-2} as the upper bound for the screw-component TD density at the surface of the LEO GaN. By combining several such images, the dislocation density can in principle be as low as ~10^5 cm^{-2}, similar to the case of LEO on GaN/Al_2O_3 substrates. [4]

Figure 2a shows that the atomic steps in the LEO region tend to form a paired structure along the $<1\bar{1}00>$ directions, which has been attributed to the geometry of the nitrogen dangling bonds at the step edges of nearly-dislocation-free GaN surfaces. [3] [42] Figure 2b shows a small-area image of sample A in which a ~2 μm^2 region consisting of such perfectly straight, paired steps

https://doi.org/10.1557/S1092578300000582 Published online by Cambridge University Press

aligned along one particular <1$\bar{1}$00> direction can be observed in the LEO region. Figure 2c shows that the steps in sample B do not have the same degree of order. In particular, step-bunching can be seen in the transition between the seed and the LEO region, whereas the same transition is essentially smooth in sample A. TEM observations (see below) and complementary AFM studies (not shown) [43] suggest that the step-bunched regions are related to dislocations with line direction parallel to the (0001) basal plane located close to the surface of the stripe.

Pure edge TDs (**b** = 1/3 <11$\bar{2}$0>) are also typically present in GaN films grown on lattice mismatched substrates, and are usually (but not systematically) revealed by small surface depressions unrelated to step terminations. Such surface depressions can be observed in Figure 2b (see arrow "E") and, to a lesser extent, in Figure 2a. The arrangement of the depressions suggests that the GaN in the seed region has a columnar structure with a grain size on the order of ~0.2 μm, which is typical for our GaN films grown on unpatterned AlN/Si(111) substrates. [43]

Cross-section TEM micrographs of samples A and B are shown in Figure 3a and 3b, respectively. In both cases the seed region has a TD density on the order of ~10^{11} cm^{-2}, consisting predominantly of pure edge dislocations. In contrast, the LEO regions have a very low density of TDs and an essentially single-crystalline microstructure. Mixed-character dislocations parallel to the basal plane with <11$\bar{2}$0> line direction are observed in both samples. In sample A these dislocations are found only in a ~1 μm-thick region above the SiO_2 mask (see white arrow in Figure 3a), whereas in sample B (Figure 3b) they are observed throughout the thickness of the LEO film. Although the physical origin of these dislocations is not fully understood, it is most likely related to the stripe morphology, that is, TDs with line direction close to the [0 0 0 1] axis can change line direction to <11$\bar{2}$0> when located in close proximity of an inclined sidewall (see e.g. Ref. [6]). Since sample A exhibits both inclined and vertical facets, a significant fraction of the TDs in the seed region remains unaffected by the sidewalls; on the contrary, the sidewalls in sample B consist of the inclined facet only and can therefore affect the TDs throughout the growth.

As reported earlier in the case of LEO of GaN on GaN/Al_2O_3 substrates, [4] [2] the *c*-planes of the LEO regions grown on Si(111) are tilted relative to that of the seed region towards the <11$\bar{2}$0> direction perpendicular to the stripe orientation. Figure 4a shows x-ray rocking curves for sample A measured along the stripe axis (<1$\bar{1}$0l>, dotted line) and perpendicular to the stripe axis (<11$\bar{2}$l>, solid line). The peak at ω-$\omega_{(0002)}$=0 for the two curves corresponds to the 0002 reflection of GaN from the seed region. The full width at half maximum for the dotted line is ~1000 arcsec as is typically observed for bulk GaN/Si(111). The two side lobes of the solid curve correspond to 0002 diffraction from the LEO regions, which have an average tilt of ~0.7°. Figure 4b shows similar curves for sample B, for which the average tilt is ~4.7°. Tilt angles of ~0.2° (Ref. [4]) and ~1° (Ref. [2]) have been recently reported for LEO GaN grown on sapphire by MOCVD and hydride vapor-phase epitaxy (HVPE), respectively. In both cases, a low-angle tilt boundary consisting of dislocations with line direction parallel to the stripe could be clearly identified between the seed and the LEO regions. On the other hand, tilt angles as large as 40° have also been reported in LEO GaN grown on sapphire by HVPE; [44] in this case the tilt angle increased continuously across the stripe and was tentatively related to dislocation loops in the LEO region. Figure 3 suggests that the tilt also increases progressively across the LEO regions is samples A and B and is accommodated by the edge dislocations with line direction parallel to the stripe direction that are distributed in the LEO region.

Figure 5 shows room-temperature PL spectra of samples A and B. For both samples the GaN band-edge emission at ~365.8 nm and an intense deep level-related band centered at 570 nm are observed. It is typical for uncoalesced LEO GaN stripes to exhibit yellow luminescence, which gradually decreases as the growth proceeds towards complete coalescence. [45] This is most likely related to the large initial growth rate resulting from the enhancement of the Ga precursor supply from the mask regions. [45] The band-edge emission is associated with free excitons [46] and suggests that the GaN is under tensile stress, as is commonly observed for growth on silicon substrates. [25] [46] In this experiment the emission from both the seed and the LEO regions was measured, therefore the contributions from the different regions could be not separated (see e.g. Ref. [7]).

Figure 6a shows a plan-view SEM micrograph of sample A; Figure 6b and 6c show monochromatic CL images of the same region with the monochromator set at the band edge emission of GaN. The dark areas in the seed region are associated with threading dislocations, which have been postulated to act as non-radiative recombination centers. [38] The LEO regions show spatially uniform luminescence, which is consistent with a low density of electrically active defects and corroborates previous indications that the threading dislocations have a deleterious effect on the photoluminescence intensity in GaN. [7] [8] [10] Dark straight lines parallel to the <11$\bar{2}$0> directions are observed both in the seed region and the LEO regions. As indicated by Figure 6a,

https://doi.org/10.1557/S1092578300000582 Published online by Cambridge University Press

these electrically active features do not seem to correspond to any morphological defects at the surface of the LEO stripes. However, their orientation corresponds to the slip planes in GaN ($\{1\bar{1}00\}$) and it therefore seems plausible that they correspond to slip bands resulting from partial plastic relaxation of the GaN stripes. Since the LEO GaN stripe is grown from a thin AlN buffer layer (as opposed to a fully-coalesced, planar GaN film), it is also possible that these features correspond to stacking faults. Sample B also exhibits luminescence in the CL experiment (not shown) but the interpretation of the contrast is complicated by light extraction issues related to the rough morphology of the inclined sidewalls.

4 Discussion

Although the LEO of GaN on AlN/Si(111) substrates occurs in a very similar way as on GaN/Al_2O_3 substrates, significant structural differences can be noted, as discussed below.

4.1 Stripe morphology and microstructure

Figure 1 indicates that the LEO stripes grown on AlN/Si(111) are bound at least in part by inclined sidewalls. For identical pattern and growth conditions, the LEO growth on GaN/Al_2O_3 substrates would result in vertical sidewalls only (see e.g. Refs [3], [4]). In addition, the sidewall morphology appears to depend on the thickness of the AlN buffer layer (compare Figure 1a and 1b). The two effects are reproducible and are not associated with any change in the controllable growth parameters, such as susceptor temperature, input flow rates, and history of the growth chamber.

Another particularity of the growth on Si(111) is that, unlike the equivalent process on GaN/Al_2O_3 substrates, which appears to be extremely robust, the LEO stripes grown on AlN/Si(111) undergo a gradual degradation as the growth duration is increased. The affected stripes exhibit regions of rough morphology associated with an erosion of the SiO_2 mask and the underlying silicon substrate near the edge of the stripes, as well as a significant loss of growth selectivity. The rough regions are sometimes bounded by cracks in the LEO stripe (cracking is discussed below). The degradation appears to be essentially independent of the thickness of the SiO_2 mask, but is strongly dependent on the thickness of the AlN layer. For example, approximately 50% of the surface of the wafer is degraded in structures such as sample A (60 nm-thick AlN buffer) after two hours of growth, whereas wafers with 180 nm-thick buffers can be grown to full coalescence without any signs of degradation.

Although the exact cause of this degradation phenomenon is unknown, its relationship with the AlN buffer thickness suggests that it involves chemical reactions between the precursors and silicon out-diffusing from the Si(111) wafer through the buffer layer. Recent results have shown that silicon doping affects the configuration of surface steps [47] [48] during growth of planar GaN films, as well as the morphology of GaN pyramids during selective-area growth and LEO. [49] Based on these results, it is reasonable to assume that the differences in facet morphology between samples overgrown using different substrates (GaN/Al_2O_3 and AlN/Si(111)) and different buffer thicknesses can be explained at least in part by the presence of silicon out-diffusing from the substrate at a rate that decreases as the AlN buffer thickness is increased. The exact mechanisms of this process, for example, whether the silicon actually diffuses through the GaN stripe, the SiO_2 mask, or both, are not known at this time but do not affect the conclusion in a fundamental way. Further studies on the effect of intentional Si-doping during LEO will be published elsewhere. We note that Linthicum et al. have recently used a SiC diffusion barrier [35] to prevent degradation of the GaN stripes during growth on silicon. However our results indicate that an AlN layer alone is sufficient to prevent this degradation provided that it is sufficiently thick.

We note that the polarity of GaN on AlN/Si(111) grown by MOCVD has not been determined. Based on the considerable body of literature on the relation between polarity and morphology in GaN, [50] significant morphological differences should be expected between Ga-face LEO GaN and N-face LEO GaN. Our preliminary experiments with the LEO of GaN by MOCVD on thick N-face GaN grown on sapphire by molecular beam epitaxy have shown that the stripe morphology is considerably rougher than for Ga-face LEO GaN, which suggests that LEO GaN on AlN/Si(111) is of Ga-face polarity. Work towards the explicit determination of the polarity is underway.

Finally, other process parameters could be affected by the choice of substrate. For example, the better thermal conductivity of silicon compared to sapphire (124 vs 25 W/mK at 298K) could result in a difference in substrate temperature, which in turn would affect the stripe morphology. [39] Such effects could conceivably explain the difference in facet morphology between GaN/Al_2O_3 and AlN/Si(111) substrates; however they do not explain the effect of the AlN buffer thickness.

4.2 Thermal mismatch

Although the cracking issue is not well documented in other studies, it is common to observe cracking for bulk GaN on Si grown by MOCVD. [23] [43] [51] This is to be expected since the thermal expansion mismatch between GaN ($\alpha = 5.6\times10^{-6}$ K^{-1} (a axis)) and Si (α =

https://doi.org/10.1557/S1092578300000582 Published online by Cambridge University Press

3.6×10^{-6} K^{-1}) causes GaN to be under tensile stress after cooldown. Our PL and CL data (Figs. 5 and 6) indeed show that samples A and B are under tensile stress, and similar PL peak energies were also observed for planar GaN grown on Si(111). [25] [43] [46]

Cracking occurs along the three equivalent $\{1\bar{1}00\}$ planes in planar films. However, for uncoalesced GaN stripes the normal stresses on the three $\{1\bar{1}00\}$ planes are not equivalent because of the finite lateral extent of the stripes. [b] Sample B exhibited cracks on the $\{1\bar{1}00\}$ planes perpendicular to the stripe direction. The spacing between the cracks was ~50 μm. Sample A exhibited a much lower crack density, with the distance between cracks on a given stripe being in excess of ~300 μm. Thus the average crack-free area for sample A was on the order of 3000 μm^2, similar to that observed for planar GaN/AlN/Si(111). [43] Although these results suggest that the stress was lower in sample A than in sample B, it is likely that the cracking was enhanced in sample B due to stress concentration associated with the facetted, inclined sidewalls (as opposed to the smooth $\{11\bar{2}0\}$ facet at the base of sample A). Additionally, cracking might have been enhanced due to hardening effects related to the pinning of slip mechanisms by the larger density of extended defects in the LEO region in sample B. Although the origin of the dark lines in sample A (Figure 6) is unknown, they could indicate the onset of plastic relaxation.

Although no modeling of the thermal stress in LEO GaN was performed in our studies, our experimental results indicate that cracking depends on most growth and processing parameters, such as the thickness of AlN buffer layer (as discussed above) and of the SiO_2 mask, pattern geometry, V/III ratio, and growth temperature. A more systematic study of the effect of processing parameters on the thermal strain in GaN/AlN/Si(111) is underway.

5 Conclusions

We have obtained LEO GaN stripes on Si(111) substrates using a thin AlN buffer layer and characterized their structural and optical properties. A reduction in threading dislocation density of 3-4 orders of magnitude was corroborated by AFM, TEM, and CL measurements. The AlN buffer thickness was shown to affect the stripe morphology and, in turn, the microstructure and the extent of cracking in the LEO stripes. The stripe morphology and growth selectivity gradually degrade as the growth duration is increased; a 180 nm-thick AlN buffer was shown to prevent degradation, such that full coalescence can be achieved on a 40 μm-period pattern. Further studies on the electrical properties of the LEO GaN on Si(111) are underway.

ACKNOWLEDGMENTS

This work was supported by the Office of Naval Research through a contract supervised by Dr. C. Wood and made use of the MRL Central Facilities supported by the NSF under award DMR-9123048. HM acknowledges financial support from NSERC (Canada). PF ackowledges financial support from a National Defense Science and Engineering Graduate Fellowship provided by ONR.

REFERENCES

[a] For a microstructural study of AlN/Si(111) films, see e.g. Ref. [37]

[b] For all samples analyzed so far, cracking along the diagonal {1;;onebar; 00} planes occurs only when the stripes come in contact and form a coalesced films; the situation then becomes similar to that of a planar film.

[1] Tsvetanka S. Zheleva, Ok-Hyun Nam, Micheal D. Bremser, Robert F. Davis, *Appl. Phys. Lett.* ***71*** , 2472-2474 (1997).

[2] A Sakai, H Sunakawa, A Usui, *Appl. Phys. Lett.* ***71*** , 2259-2261 (1997).

[3] Hugues Marchand , J.P. Ibbetson, Paul T. Fini , Peter Kozodoy , S. Keller, Steven DenBaars , J. S. Speck, U. K. Mishra, *MRS Internet J. Nitride Semicond. Res.* ***3*** , 3 (1998).

[4] H Marchand, XH Wu, JP Ibbetson, PT Fini, P Kozodoy, S Keller, JS Speck, SP DenBaars, UK Mishra, *Appl. Phys. Lett.* ***73*** , 747-749 (1998).

[5] O-H Nam, MD Bremser, TS Zheleva, RF Davis, *Appl. Phys. Lett.* ***71*** , 2638-2340 (1997).

[6] A Sakai, H Sunakawa, A Usui, *Appl. Phys. Lett.* ***73*** , 481-483 (1998).

[7] SF Chichibu, H Marchand, MS Minski, S Keller, PT Fini, JP Ibbetson, T Deguchi, T Sota, S Nakamura, unpublished.

[8] JA Freitas, O-H Nam, RF Davis, GV Saparin, SK Obyden, *Appl. Phys. Lett.* ***72*** , 2990-2992 (1998).

[9] X Li, SG Bishop, JJ Coleman, *Appl. Phys. Lett.* ***73*** , 1179-1181 (1998).

[10] SJ Rosner, G Girolami, H Marchand, PT Fini, JP Ibbetson, L Zhao, S Keller, UK Mishra, SP DenBaars, JS Speck, unpublished.

[11] P Kozodoy, JP Ibbetson, H Marchand, PT Fini, S Keller, SP DenBaars, JS Speck, UK Mishra, *Appl. Phys. Lett.* ***73*** , 975-977 (1998).

[12] T Mukai, K Takekawa, S Nakamura, *Jpn. J. Appl. Phys.* ***37*** , L839-L841 (1998).

[13] C Sasaoka, H Sumakawa, A Kimura, M Nido, A Usui, A Sakai, *J. Cryst. Growth* ***189/190*** , 61-66 (1998).

[14] R Vetury, H Marchand, JP Ibbetson, PT Fini, S Keller, JS Speck, SP Denbaars, UK Mishra, edited by:, Y Hirayama, unpublished.

[15] G Parish, S Keller, P Kozodoy, JP Ibbetson, H Marchand, PT Fini, SB Fleisher, SP DenBaars, UK Mishra, unpublished.

[16] S Nakamura, M Senoh, S Nagahama, N Iwasa, T Yamada, T Matsushita, H Kiyoku, Y Sugimoto, T Kozaki, H Umemoto, M Sano, K Chocho, *Appl. Phys. Lett.* ***72*** , 211-213 (1998).

[17] S. Guha, N. A. Bojarczuk, *Appl. Phys. Lett.* ***72*** , 415-417 (1998).

[18] A. Osinsky, S. Gangopadhyay, J. W. Yang, R. Gaska, D. Kuksenkov, H. Temkin, I. K. Shmagin, Y. C. Chang, J. F. Muth, R. M. Kolbas, *Appl. Phys. Lett.* ***72*** , 551-553 (1998).

[19] K. S. Stevens, M. Kinniburgh, R. Beresford , *Appl. Phys. Lett.* ***66*** , 3518-3520 (1995).

[20] T. L. Chu, *J. Electrochem.Soc.* ***118*** , 1200 (1971).

[21] H. M. Manasevit, F. M. Erdmann, W. I. Simpson, *J. Electrochem.Soc.* ***118*** , 1864 (1971).

[22] T Lei, TD Moustakas, *Mater. Res. Soc. Symp. Proc.* ***242*** , 433-439 (1992).

[23] T Takeuchi, H Amano, K Hiramatsu, N Sawaki, I Akasaki, *J. Cryst. Growth* ***115*** , 634-638 (1991).

[24] AJ Steckl, J Devrajan, C Tran, RA Stall, *Appl. Phys. Lett.* ***69*** , 2264-2266 (1996).

[25] A Watanabe, T Takeuchi, K Hirosawa, et al., *J. Cryst. Growth* ***128*** , 391-396 (1993).

[26] P. Kung, A. Saxler, X. Zhang, D. Walker, T. C. Wang, I. Ferguson, M. Razeghi , *Appl. Phys. Lett.* ***66*** , 2958-2960 (1995).

[27] W. J. Meng, T. A. Perry , *J. Appl. Phys.* ***76*** , 7824-7828 (1994).

[28] A. Ohtani, K. S. Stevens, R. Beresford , *Appl. Phys. Lett.* ***65*** , 61-63 (1994).

[29] M Godlewski, JP Bergman, B Monemar, U Rossner, A Barski, *Appl. Phys. Lett.* ***69*** , 2089-2091 (1996).

[30] J. W. Yang, C. J. Sun, Q. Chen, M. Z. Anwar, M. A. Khan, S. A. Nikishin, G. A. Seryogin, A. V. Osinsky, L. Chernyak, H. Temkin, C. hu, S. Mahajan, *Appl. Phys. Lett.* ***69*** , 3566 (1996).

[31] N. P. Kobayashi, J. T. Kobayashi, P. D. Dapkus, W. J. Choi, A. E. Bond, X. Zhang, D. H. Rich, *Appl. Phys. Lett.* ***71*** , 3569-3571 (1997).

[32] Y Nakada, I Aksenov, H Okumura, *Appl. Phys. Lett.* ***73*** , 827-829 (1998).

[33] H Marchand, N Zhang, L Zhao, Y Golan, PT Fini, JP Ibbetson, S Keller, SP DenBaars, JS Speck, UK Mishra, edited by:, Y. Hirayama, unpublished.

[34] Y Kawaguchi, Y Honda, M Yamaguchi, K Hiramatsu, N Sawaki, edited by:, Y Hirayama, unpublished.

[35] K. J. Linthicum et al., to be published in MRS Internet J. Nitride Semicond. Res.

[36] P Kung, D Walker, M Hamilton, J Diaz, M Razeghi, *Appl. Phys. Lett.* ***74*** , 570-572 (1999).

[37] M. Zhou, N.R. Perkins, E. Rehder, T.F. Kuech, and S.E. Babcock, Mater. Res. Soc. Symp. Proc. 482, 185 (1998)

[38] SJ Rosner, EC Carr, MJ Ludowise, G Girolami, HI Erikson, *Appl. Phys. Lett.* ***70*** , 420-422 (1997).

[39] H Marchand, JP Ibbetson, PT Fini, S Keller, SP DenBaars, JS Speck, UK Mishra, *J. Cryst. Growth* ***195*** , 328-332 (1998).

[40] O-H Nam, T. S. Zheleva, MD Bremser, RF Davis, *J. Electron. Mater.* ***27*** , 233 (1998).

[41] D. Kapolnek, X. H. Wu, B. Heying, S. Keller, B. P. Keller, U. K. Mishra, S. P. DenBaars, J. S.Speck , *Appl. Phys. Lett.* ***67*** , 1541-1543 (1995).

[42] T Nishida, T Akasaka, N Kobayashi, *Jpn. J. Appl. Phys.* ***37*** , L459 (1998).

[43] H. Marchand, unpublished results

[44] K Tsukamoto, W Taki, N Kuwano, K Oki, T Shibata, N Sawaki, K Hiramatsu, in , Edited by: , K Onabe, K Hiramatsu, K Itaya, Y Nakano, (Ohmsha Ltd, Tokyo, 1998) Th-P11.

[45] H Marchand, JP Ibbetson, PT Fini, XH Wu, SJ Rosner, S Keller, JS Speck, UK Mishra, SP DenBaars, unpublished.

[46] S. Chichibu, T. Azuhata, T. Sota, H. Amano, I. Akasaki, *Appl. Phys. Lett.* ***70*** , 2085 (1997).

[47] S Keller, SF Chichibu, MS Minsky, E Hu, UK Mishra, SP DenBaars, *J. Cryst. Growth* ***195*** , 258-264 (1998).

[48] XQ Shen, S Tanaka, S Iwai, Y Aoyagi, *Appl. Phys. Lett.* ***72*** , 344-346 (1998).

[49] S. Haffouz, B. Beaumont, Pierre Gibart , *MRS Internet J. Nitride Semicond. Res.* ***3***, 8 (1998).

[50] E. S. Hellman, *MRS Internet J. Nitride Semicond. Res.* ***3***, 11 (1998).

[51] S Guha, NA Bojarczuk, *Appl. Phys. Lett.* ***73*** , 1487-1489 (1998).

FIGURES

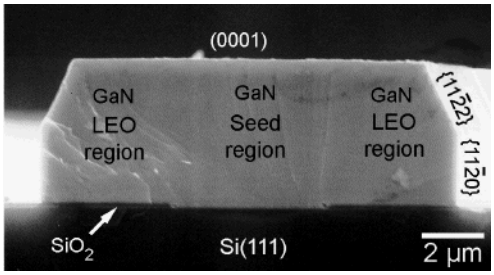

Figure 1a. Cross section SEM micrograph of a typical GaN LEO stripe on Si(111) after 60 minutes of growth: sample A, 60 nm-thick AlN.

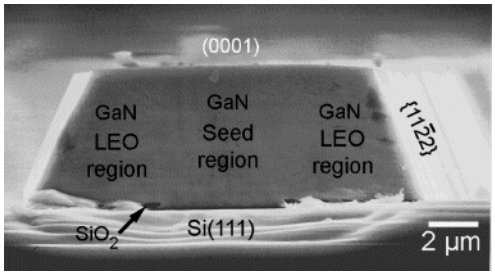

Figure 1b. Cross section SEM micrograph of a typical GaN LEO stripe on Si(111) after 60 minutes of growth: sample B, 180 nm-thick AlN.

https://doi.org/10.1557/S1092578300000582 Published online by Cambridge University Press

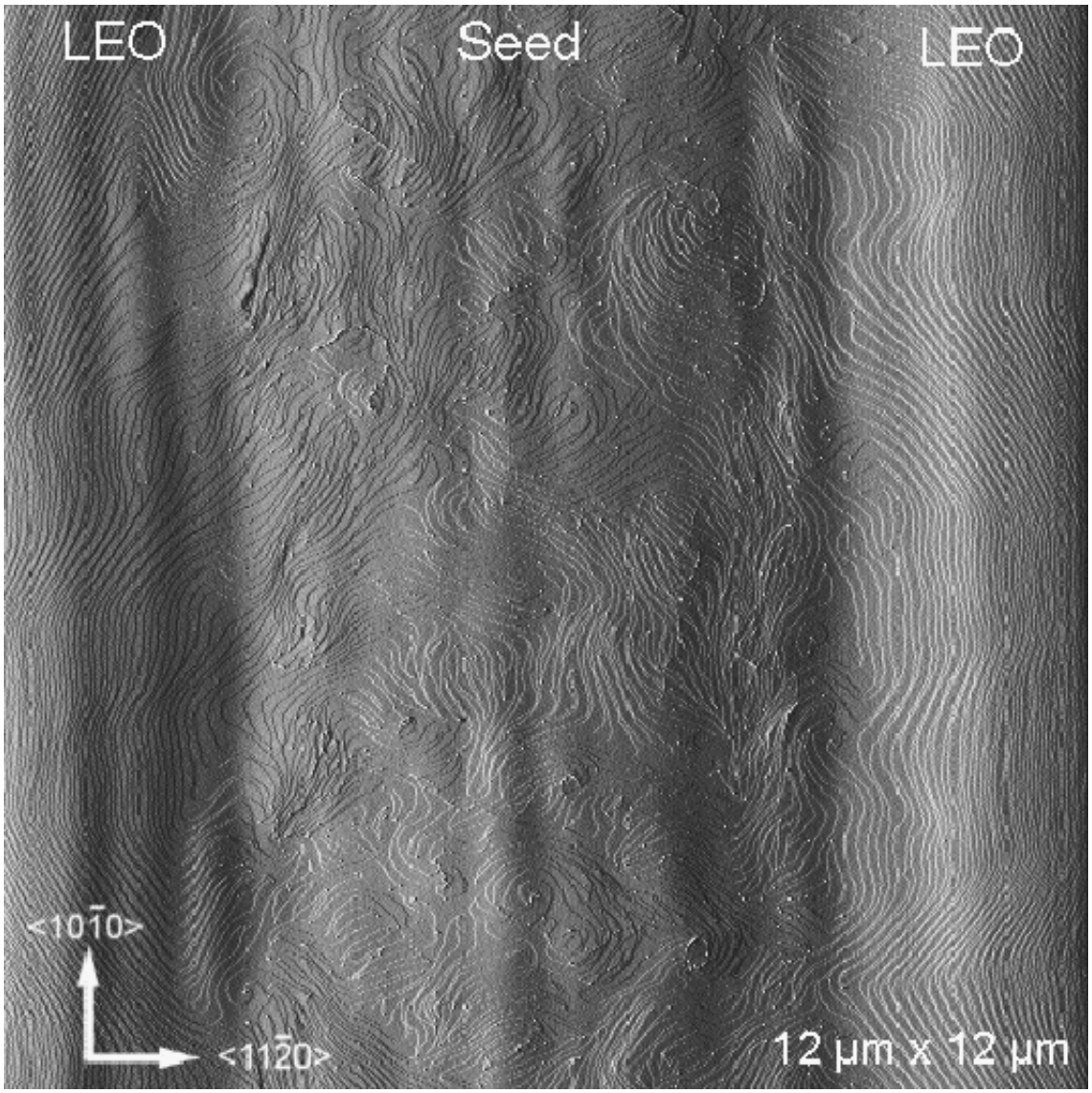

Figure 2a. Surface topography measured by tapping mode AFM: sample A, large-area scan.

https://doi.org/10.1557/S1092578300000582 Published online by Cambridge University Press

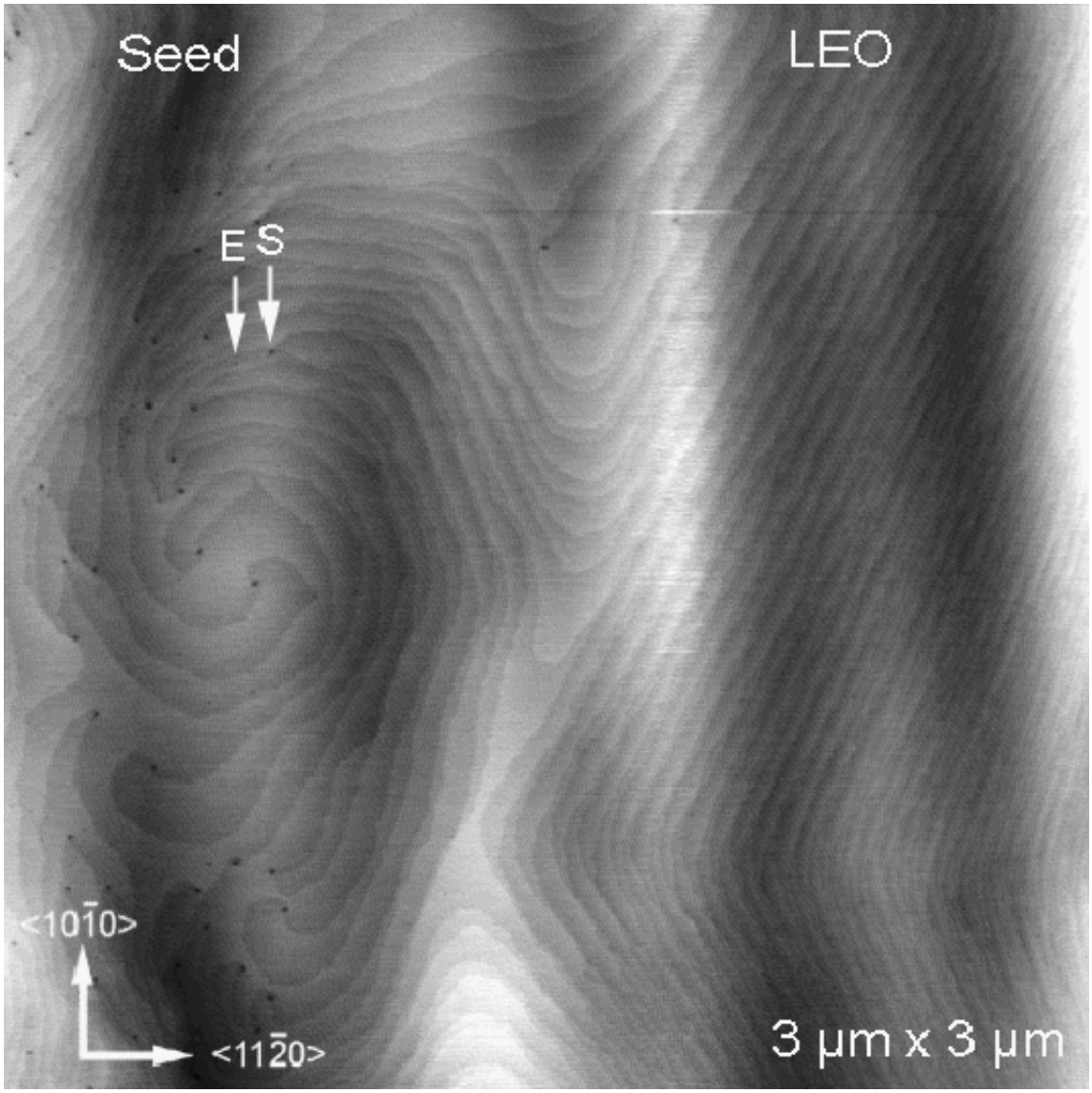

Figure 2b. Surface topography measured by tapping mode AFM: sample A, height mode. The "S" arrow indicates an instance of step termination associated with a screw-character threading dislocation intersection the surface of the film. The "E" arrow indicates an instance of a smaller surface depression typically associated with pure edge threading dislocation.

https://doi.org/10.1557/S1092578300000582 Published online by Cambridge University Press

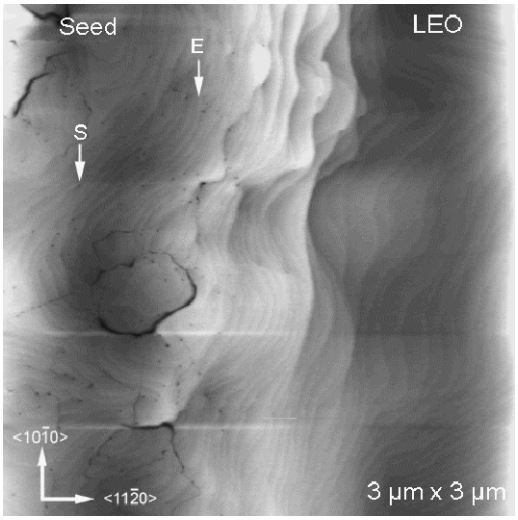

Figure 2c. Surface topography measured by tapping mode AFM: sample B, height mode. "S" and "E" arrows as in Figure 2b.

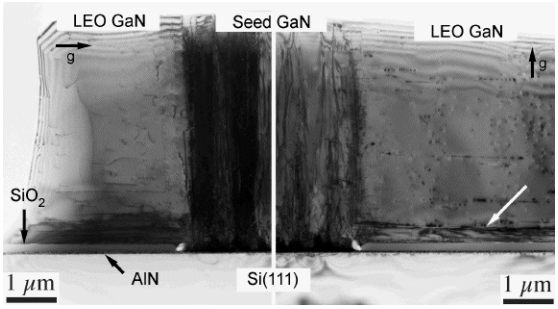

Figure 3a. Cross section bright-field TEM micrographs of sample A. The left and right panels correspond to g = 11$\bar{2}$0 and g = 0002, respectively. The irregular top and side surfaces are due to the ion milling process.

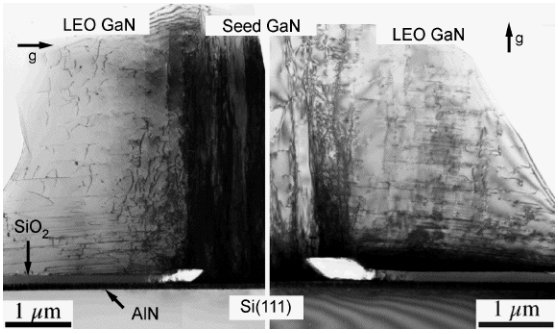

Figure 3b. Cross section bright-field TEM micrographs of sample B. The left and right panels correspond to g = 11$\bar{2}$0 and g = 0002, respectively. The irregular top and side surfaces are due to the ion milling process.

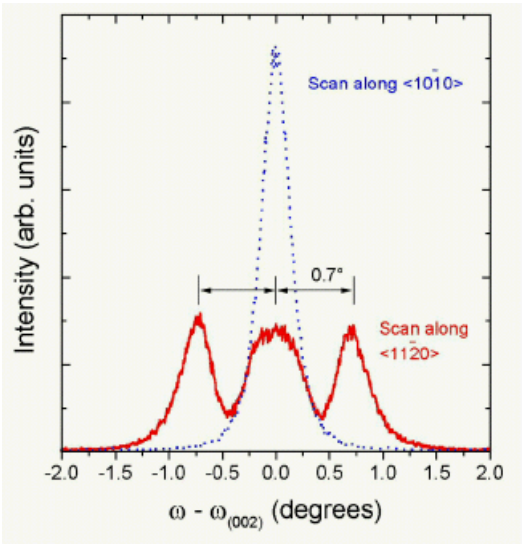

Figure 4a. X-ray rocking curves of sample A. The dotted (solid) line corresponds to an ω-scan with the stripe direction parallel (perpendicular) to the diffraction plane.

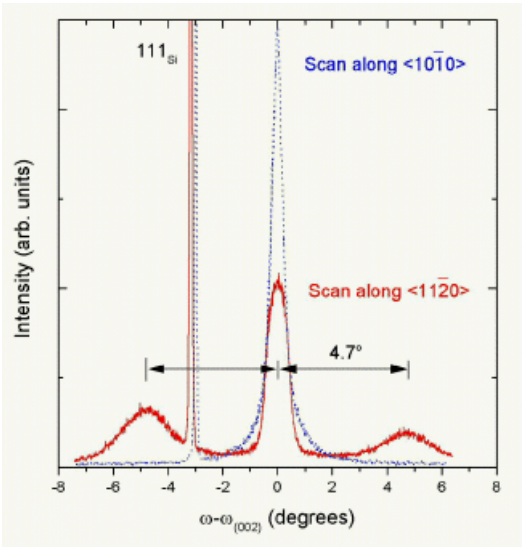

Figure 4b. X-ray rocking curves of sample B. The dotted (solid) line corresponds to an ω-scan with the stripe direction parallel (perpendicular) to the diffraction plane.

https://doi.org/10.1557/S1092578300000582 Published online by Cambridge University Press

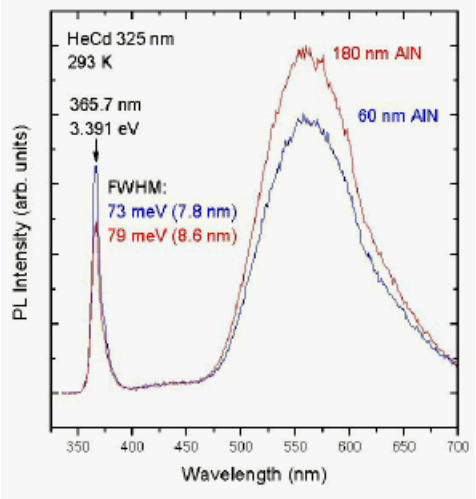

Figure 5. Room temperature PL spectra of samples A and B. In this experiment the emission from both the LEO and the seed region was collected.

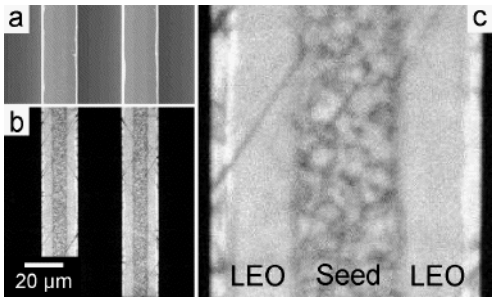

Figure 6. (a) Plan-view SEM micrograph of sample A; (b) monochromatic (λ=367 nm) CL images of the same region; (c) high magnification image of (b).

MRS Internet J. Nitride Semicond. Res. 4, 2 (1999).